ADVANCED ENGINEERING MATERIALS
www.aem-journal.com

Barium Ferrite/Carbon Nanotube Nanocomposites for Millimeter-Wave Electromagnetic Shielding Enhanced by Ferromagnetic Resonance Absorption

Brenden M. Mears, Faith M. Freeman, Yong-Kyu Yoon, and David P. Arnold*

In this work, a composite of barium ferrite (BaM) and multiwalled carbon nanotubes (CNTs) in a polymer matrix of polydimethylsiloxane (PDMS) are reported for the purpose of suppressing electromagnetic interference (EMI). Shielding is accomplished primarily through absorption, which arises from a combination of the ferromagnetic resonance (FMR) from the BaM and conductive losses from the CNTs. The composite is fabricated by mixing commercially available BaM nanoparticles and CNTs into PDMS, screen printing the mixture into molds, then curing at 80 °C in a DC magnetic field. Characterization involves placing the composite in the cross-section of a rectangular waveguide, then using a vector network analyzer (VNA) to measure scattering (S) parameters from 33–50 GHz. Using the measured S parameters, power reflected and absorbed can be calculated and used to characterize the composite's shielding effectiveness (SE), and the complex permittivity and permeability can be determined. The resulting 2.4 mm thick composite shows a peak absorption of 26.9 dB at the FMR frequency of 47.4 GHz. When normalized for thickness, the composite, on average, absorbs 11.3 dB mm^{-1} and operates at a higher frequency than other shielding composites found in the literature.

1. Introduction

The increasing usage of wireless devices generates an increasing amount of electromagnetic radiation in the ambient environment. This excess radiation can result in electromagnetic interference (EMI) which can affect sensitive devices, especially in the microwave and millimeter wave ranges.[1,2] To exacerbate this problem, electronic devices are increasingly packed closer together due to system miniaturization and increasing levels of integration, which increase the likelihood of interference.[3] Consequently, EMI is an important design consideration for aerospace,[4] defense,[1] and consumer electronics.[3] There is a wealth of prior research focused on EMI shielding materials at frequencies below 20 GHz. However, for application in 5 and 6 G consumer applications, as well as many defense and military systems, shielding materials are needed for frequencies at 20 GHz and beyond.

The most basic shielding techniques utilize metals to reflect EMI. Highly conductive metals create a large electromagnetic impedance mismatch with air, which leads to very large reflections off the metal–air interface, and little to no transmitted EMI[5]. However, reflection is not necessarily the ideal shielding mechanism, as the EMI is simply redirected and not attenuated. Other problems with metals include their high mass densities, rigidity, and susceptibility to corrosion.[1,4,6] The alternative mechanism to reflection is absorption, which attenuates EMI by converting electromagnetic energy to heat[7], as shown in **Figure 1**. To be an effective absorber, the shielding material must have high electrical and/or magnetic losses.[7,8] Strongly absorbing shielding composites with low reflection have been explored at millimeter wave frequencies, achieving over 30 dB absorption from 40 to 90 GHz.[9] However, the best performing absorbers require complex, expensive particle, and film fabrication processes. This work seeks to improve upon the field by presenting cost-effective, high frequency absorbing shields using readily available bulk materials and simple fabrication processes to achieve high levels of EM absorption. For system application and integration, ideal absorbing materials should be low density, low cost, mechanically reliable, and also manufacturable via scalable, low temperature processes.

In this work, composites made from polydimethylsiloxane (PDMS), *M*-type barium ferrite (chemical formula $BaFe_{12}O_{19}$, abbreviated as BaM) nanoparticles, and multi-wall carbon nanotubes (CNTs) are fabricated and characterized to determine both shielding properties and electromagnetic material parameters. Fabrication was performed via a screen-printing process, and characterization was performed using a rectangular waveguide and vector network analyzer (VNA). PDMS is a polymer used in microwave applications, is flexible when cured, and can be fabricated using low-temperature processes.[10] CNTs are utilized for their broadband conductive properties to create a moderately conductive, thus electrically lossy, composite.[1] BaM contributes frequency-selective magnetic loss to the composite via magnetic absorption, particularly near the ferromagnetic resonance (FMR) frequency.[11]

B. M. Mears, F. M. Freeman, Y.-K. Yoon, D. P. Arnold
Department of Electrical and Computer Engineering
University of Florida
Gainesville, Florida 32611, USA
E-mail: mearsb@ufl.edu

The ORCID identification number(s) for the author(s) of this article can be found under https://doi.org/10.1002/adem.202400084.

DOI: 10.1002/adem.202400084

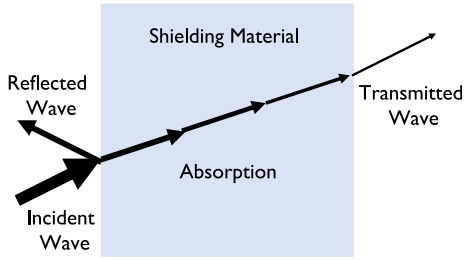

Figure 1. Electromagnetic shielding mechanisms showing an incident wave, reflected wave, and transmitted wave.

FMR in a magnetic material is the coupling between an electron's spin and an incident electromagnetic wave. FMR occurs at the electron's precession frequency, which is the FMR frequency, and results in large magnetic losses.[11] BaM is known to have an FMR frequency around 45–50 GHz depending on composite geometry and externally applied bias magnetic field.[2,10] When used for shielding applications, a composite containing BaM should behave similarly to a band stop filter, as EMI will be most strongly attenuated at and around the FMR frequency while being transmitted at other frequencies. It is also important to note that the FMR frequency of BaM overlaps with the higher frequencies of the fifth generation (5 G) spectra. This makes BaM an excellent candidate for 5 G EMI shields and devices.

These shielding composites are also characterized to determine key material parameters such as complex permittivity and permeability. Understanding the material parameters gives a greater insight into how the composites will respond at different frequencies and opens potential uses in other applications. Existing characterization methods include commercially available hardware and software modules for VNAs that can yield permittivity, permeability, and loss tangents,[12] but characterization also be performed manually through algorithms utilizing the measured S parameters of loaded transmission lines. These algorithms include Baker–Jarvis[13] and Nicolson–Ross–Weir (NRW)[6] among others. In this work, parameter extraction is performed using the NRW method due to its compatibility with the measurement method and its simplicity in implementation, i.e., no additional hardware/software needed.

The objective of this work is to develop polymer-based composites for the purpose of millimeter wave EMI shielding. Specifically, highly absorbing composites with broadband and frequency-selective properties are explored in Q Band frequencies (33–50 GHz), which are much higher than commonly found in published literature. This frequency band also presents considerable applications for this composite in improving the electromagnetic compatibility of 5 G devices.

2. Materials and Methods

2.1. Fabrication

Sample fabrication utilizes a screen-printing process,[10,14] and is detailed in the process flow in **Figure 2**.

The PDMS (Sylgard 184) is mixed in a 10:1 ratio by weight of base to curing agent as recommended by the manufacturer. Next, the desired concentrations of electromagnetic particles are mixed in. These particles include BaM nanoparticles of 99.5% purity with an average particle size of 500 nm (Nanostructured & Amorphous Materials, Inc.) and multiwalled CNTs with 40-60 nm diameter and 5–15 μm in length (Tokyo Chemical Industry). The relatively large diameter of the CNTs results in a larger band gap and thus a higher conductivity, as they are considered metallic as compared to semiconducting CNTs. After mixing in the filler materials at various weight percentages (specific below), the composite is placed in a vacuum desiccator for 15 min to remove any bubbles in the composite. Due to the high viscosity of the mixtures, they generally must be screen printed into the mold as

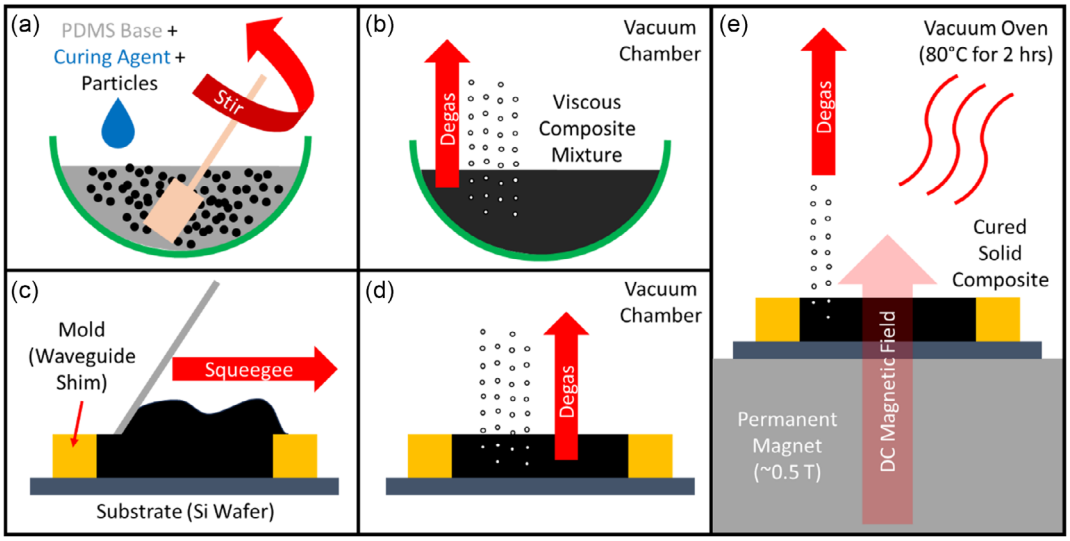

Figure 2. Process flow for fabricating shielding composites. a) PDMS base, PDMS curing agent, and particles are mixed, b) viscous mixture is placed in a vacuum chamber to degas, c) mixture is screen printed into the mold (WR-22 waveguide shim), d) mixture is again placed in a vacuum chamber to degas, and e) mixture is cured in a vacuum oven in the presence of a DC magnetic field.

opposed to being poured in. The molds used here are WR-22 rectangular waveguide shims that dimensionally match the waveguide used for testing. The WR-22 is 5.69 mm by 2.84 mm in cross section, with three different shim thicknesses used: 2.42, 1, and 0.5 mm. Waveguide shims function excellently as molds, as the finished composite sample is the exact size of the cross section. Having the composite fully fill the cross section of the waveguide is critical for obtaining accurate electromagnetic measurements. These sizes are chosen to determine shielding effectiveness as a function of sample thickness, and only the 0.5 mm shim is used for the NRW method, to ensure the sample thickness is less than a half wavelength for all measurement frequencies. After screen printing, the composites are vacuum desiccated again for 15 min to degas. Finally, the sample is placed in a vacuum oven to cure. The composite is cured on top of a permanent magnetic with a surface magnetic field of roughly 0.5 T. The magnetic field is used to align the magnetic dipoles of the BaM nanoparticles and create a self-biased composite, which results in greater FMR absorption compared to unaligned samples.[14] The samples are cured in a vacuum oven (Isotemp 281 A),to further reduce bubbles, at 80 °C for 2 h.

2.2. Measurement and Characterization

Samples of the composites containing 60 wt% BaM and 1.7 wt% CNTs were imaged by SEM (FEI Helios G4 PFIB CXE Dual Beam) as shown in **Figure 3**. The electromagnetic properties of the composites are characterized via insertion into the cross section of a WR-22 rectangular waveguide (Millimeter Wave Products Inc) and subsequent measurement of the scattering (S) parameters. Before each measurement, a two-port calibration is performed on the waveguide using a calibration kit (Q11644A) and VNA (Agilent E8361A) such that the calibration plane is moved up to the front and back faces of the sample under test. Calibration is done such that the coaxial cables and waveguide lengths have been deembedded, and only the sample properties affect the measurements. Then, a sample holder (waveguide shims of different lengths) containing the composite is placed between the two waveguide sections. The VNA then sweeps in frequency from 33 to 50 GHz, the operating range of the WR-22. A diagram of this rectangular waveguide method is shown in **Figure 4**.

With the S parameters obtained across the frequency range, shielding effectiveness (SE) in dB can be calculated according to the equations

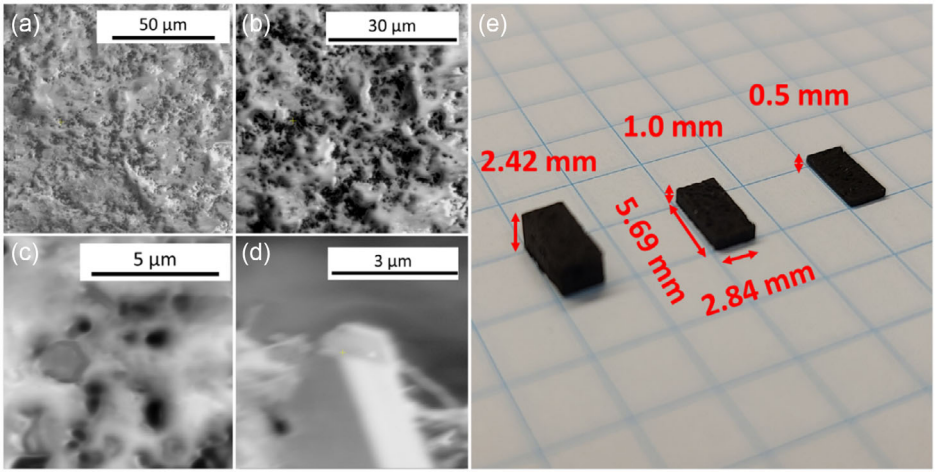

Figure 3. SEM images of a) composite surface at 50 µm scale, b) composite surface at 30 µm scale, c) view of BaM nanoparticles on composite surface, d) view of CNTs on composite surface, and e) optical image of composite samples.

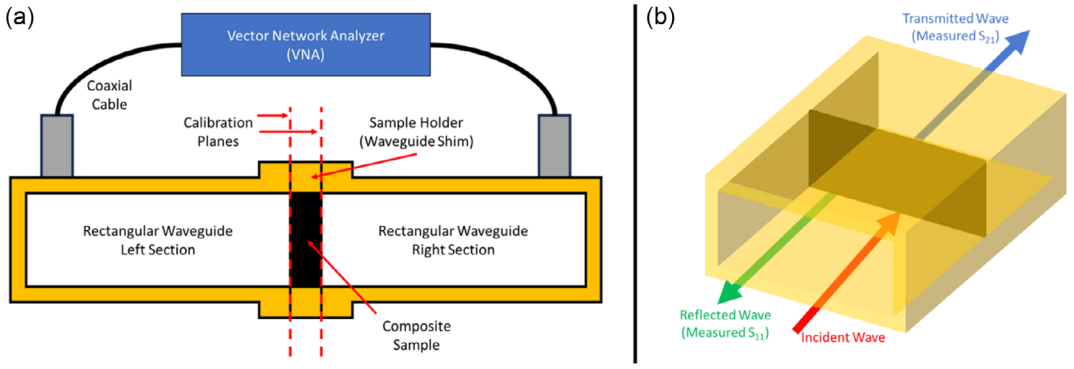

Figure 4. a) Diagram of rectangular waveguide measurement method. b) Diagram of wave/composite interaction inside the rectangular waveguide.

$$\mathrm{SE} = 20 * \log_{10}\left(\frac{E_i}{E_t}\right) = -10 * log_{10}|S_{21}|^2 = \mathrm{SER} + \mathrm{SEA} \quad (1)$$

$$\mathrm{SER} = -10 * \log_{10}(1 - |S_{11}|^2) \quad (2)$$

$$\mathrm{SEA} = -10 * \log_{10}\left(\frac{|S_{21}|^2}{1 - |S_{11}|^2}\right) \quad (3)$$

where E_i is the incident electric field magnitude, E_t is the transmitted electric field magnitude, and S_{11} and S_{21} are two of the measured S parameters. SE is the total shielding effectiveness and is a measure of the incident wave power compared to the transmitted wave power. SE is also expressed as the sum of the contributions of the shielding effectiveness from absorption (SEA) and reflection (SER). Physically, SER is the power reflected by the shield, and SEA is the power absorbed by the shield after the reflection.[1–4] SEA is the desired shielding component for this application, so it should be maximized, and SER minimized. While there is no exact SE, SEA, or SER value that determines an effective EMI shield, there are generally accepted thresholds. For absorbing shields, SEA, or power absorption in general, should be at least 10 dB (90%),[6–8] or even 20 dB (99%).[1,12] SER should then be minimized such that is significantly smaller than SEA.

The NRW method was then used to calculate complex permittivity and permeability to further characterize the composites. The NRW method is a non-iterative algorithm in which transmission and reflection information, provided by directly measured S parameters, is used to calculate the complex permittivity and permeability of a material under test.[15–17] The NRW method lends itself very nicely to characterization via rectangular waveguides but requires that the sample is below a half wavelength long (ideally a quarter wavelength or shorter) and that the sample completely fills the cross section.[18] In this work, the 0.5 mm thick samples are used in the NRW method, as the 1 and 2.42 mm samples are too long for all tested materials to remain under a half wavelength across the measured spectrum. These sample lengths proved to be too long due primarily to the BaM and CNTs increasing the refractive index thus decreasing the wavelength inside the composites.

3. Results and Discussion

3.1. Shielding Effectiveness

In **Figure 5**, SEA is plotted as the solid blue trace, and SER is the dotted red trace. SEA is the power (in dB) absorbed by the composite, and SER is the power (in dB) reflected by the composite. The FMR frequency will be determined by the frequency at which SEA peaks in magnetic composites.

Initially, 100% PDMS composites were fabricated to determine the viability of PDMS as a composite matrix material in the microwave range. The results in Figure 5a–c show that PDMS does not significantly contribute to absorption, with all PDMS composites below 1 dB of SEA, or reflection, with all PDMS composites below 2.1 dB of SER. PDMS will be used as a relatively RF-transparent polymer serving as a matrix for absorbing particles.

Next, PDMS composites consisting of 70 wt% BaM are fabricated and characterized. The concentration of 70 wt% was chosen to maximize the BaM nanoparticle load, as the mixture becomes too viscous to screen print at higher concentrations. The results for this composite are shown in Figure 5d–f. The 2.42 mm thick composite of 70 wt% BaM in Figure 5f shows an absorption peak of 10.9 dB at an FMR frequency of 47.6 GHz. It is also important to note this BaM composite reflected 1.11 dB of power at its FMR frequency. Across the entire measured spectrum, this BaM composite reflected less than 3.5 dB of power.

Composites of 7.4 wt% CNTs were fabricated and characterized to determine the shielding effectiveness of CNTs. The concentration of 7.4 wt% was chosen to maximize the CNT load, as the mixture becomes too viscous to screen print at higher concentrations. The results for this composite are plotted in Figure 5g–i. The 2.42 mm thick 7.4 wt% CNTs composite plotted in Figure 5i shows excellent broadband absorption properties with an average of 40.1 dB across the measured spectrum. This absorption is a result of electrical losses due to the broadband AC conductivity inherent to CNTs. These electrical conduction losses are desirable and can complement the magnetic losses due to FMR in BaM. The power reflected by this composite is very low in comparison to power absorbed with a mean 3.09 dB of power reflected across the measured spectrum.

When using electrically conductive CNTs in a composite, percolation theory should be considered. Percolation theory indicates that a certain concentration of CNTs will lead to the formation of a percolating network above which there is a large increase in the DC conductivity. The minimum conductivity needed for a good EMI shield is 0.01 S cm^{-1}.[1] For the purposes of EMI shielding, the percolation threshold should be met, or surpassed, as conductive losses will contribute to absorption. Fundamentally, percolation threshold for a composite containing CNTs is based on factors such as CNT concentration, CNT aspect ratio, and how well the CNTs are dispersed in the composite.[19] The 7.4 wt% CNTs composite corresponds to a volume concentration of 4.7 vol% CNTs, and the average aspect ratio of the CNTs is 200. When comparing these values to the findings in,[19] and observing a very high average absorption of 42.6 dB, it can be concluded that the concentration of 7.4 wt% CNTs surpasses the percolation threshold.

Composites containing both BaM and CNTs are fabricated consisting of 60 wt% BaM with 1.7 wt% CNTs to evaluate the combination of electric and magnetic losses. The 60 wt% BaM and 1.7 wt% CNTs concentrations were chosen, as combining 70 wt% BaM and 7.4 wt% CNTs results in a mixture that is too viscous to screen print. To maintain a mixture viscosity that was printable, the CNT and BaM concentrations were reduced. A compromise was found at 60 wt% BaM + 1.7 wt% CNTs, which yielded a workable mixture that allowed for uniform sample fabrication. Figure 5j–l shows the power absorbed and reflected for these composites of 60 wt% BaM + 1.7 wt% CNTs. The 2.42 mm composite in Figure 5L has an absorption peak of 26.9 dB at 47.4 GHz. Based on the shielding results from the BaM-only and CNT-only samples, the CNTs contribute a high broadband absorption, while the BaM provides an additional peak on top of the broadband absorption from the CNTs. The 1.7 wt% CNTs concentration in this composite can also be concluded to be above the percolation threshold when observing the broadband absorption and comparing the CNT concentration and aspect ratio to the findings in.[19] Although the peak absorption value

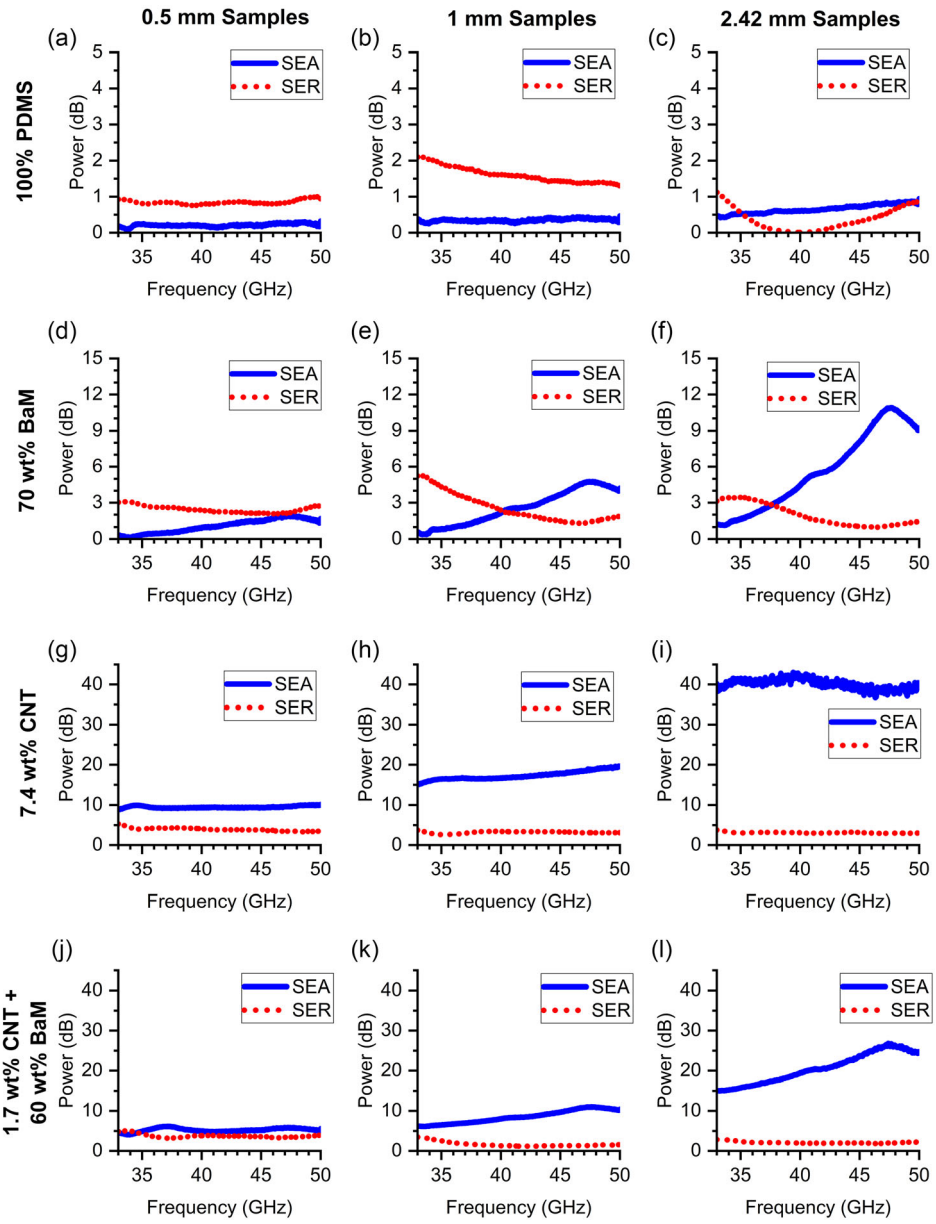

Figure 5. SEA and SER results for 100% PDMS samples of a) 0.5 mm, b) 1 mm, c) 2.42 mm thickness, 70 wt% BaM samples of d) 0.5 mm, e) 1 mm, f) 2.42 mm thickness, 7.4 wt% CNT samples of g) 0.5 mm, h) 1 mm, i) 2.42 mm thickness, and 60 wt% BaM + 1.7 wt% CNT samples of j) 0.5 mm, k) 1 mm, l) 2.42 mm thickness.

of this BaM + CNTs composite in Figure 5l is less than the broadband absorption of the CNTs composite in Figure 5i, this composite is desirable in that it shows frequency selectivity. This frequency selectivity results in behavior similar to a band-stop filter, as frequencies around 47.4 GHz are attenuated more strongly than other frequencies. The 2.42 mm composite also demonstrates low SER with 1.94 dB of power reflected at the FMR frequency and less than 3dB power reflected across the measured spectrum. The peak absorption value of the 2.42 mm composite of 26.9 dB meets the SEA requirement of >20 dB and is also significantly greater than the reflected power of 1.94 dB.

Table 1 shows the absorption values of each composite normalized by the three different lengths of the composites, where the results are in dB absorbed per millimeter of sample thickness. The values for the composites based on FMR absorption (70 wt% BaM and 60 wt% BaM + 1.7 wt% CNTs) are taken as their peak absorption values, whereas the non-magnetic (100% PDMS and 7.4 wt% CNTs) composites are taken as their averages across the spectrum due to their broadband properties. The average of the three composite lengths is taken and yields a figure of merit (FoM) for each composite type in terms of dB of power absorbed per composite length. This FoM is selected, as SEA depends on both the composite's composition and thickness.

Table 1. Normalized absorption of composites in dB/mm.

Thickness [mm]	100% PDMS	70 wt% BaM	7.4 wt% CNTs	60 wt% BaM + 1.7 wt% CNTs
2.42	0.27	4.51	16.6	11.1
1	0.35	4.78	17.3	11.0
0.5	0.42	3.86	19.0	11.8
Average	0.35	4.38	17.6	11.3

This can be seen in the propagation constant γ in (4):

$$\gamma = \alpha + j\beta = j\omega\sqrt{\mu\varepsilon} \tag{4}$$

where α is the attenuation constant in Np/m, and β is the phase constant in rad/m. The propagation constant defines how an electromagnetic wave propagates through a material, where the attenuation constant (real part) determines the material's absorption/attenuation per unit length and the phase constant (imaginary part) determines the phase change of the wave per unit length. By dividing the SEA of a composite by its thickness, the normalized attenuation of the composition can be determined independent of thickness.

(4) can be expanded to include the real and imaginary parts of permittivity and permeability

$$j\omega\sqrt{\mu\varepsilon} = \frac{j\omega}{c}\sqrt{(\mu' - j\mu'')(\varepsilon' - j\varepsilon'')} \tag{5}$$

where c is the speed of light in a vacuum, μ' and μ'' are the real and imaginary relative permeability, respectively, and ε' and ε'' are the real and imaginary relative permittivity, respectively. For the case of a lossless material, ε'' and μ'' are zero, resulting in a purely imaginary propagation constant with an attenuation constant of zero. Larger imaginary components of permeability and permittivity contribute to higher material losses, thus increasing the attenuation constant and SEA.

3.2. Complex Permittivity and Permeability

The NRW method was then employed to obtain the complex permittivity and permeability for the four PDMS composite mixtures. The resulting complex permittivity, complex permeability, and loss tangents are shown in **Figure 6**. To improve the accuracy of the NRW method, the complex relative permeability was forced to unity for the non-magnetic composites:[18] the PDMS and 7.4 wt% CNT samples. When allowing the permeability to vary for the non-magnetic composites, the real part showed deviation from unity (1) up to 30%, and the imaginary part was on the same order of magnitude as the magnetic samples. This is likely due to the NRW method being susceptible to noise and phase errors in the VNA, especially in low loss materials.[18] It is also important to note the large peak in the complex permittivity of the 7.4 wt% CNT sample around 34 GHz. This is due to experimental measurement error and does not indicate a resonance related to the presence of CNTs, as there is no similar feature in the 60 wt% BaM + 1.7 wt% CNT sample.

The complex permeability plots demonstrate expected FMR behavior from BaM in the magnetic samples. The real part is greater than unity in frequencies below FMR, crosses unity at

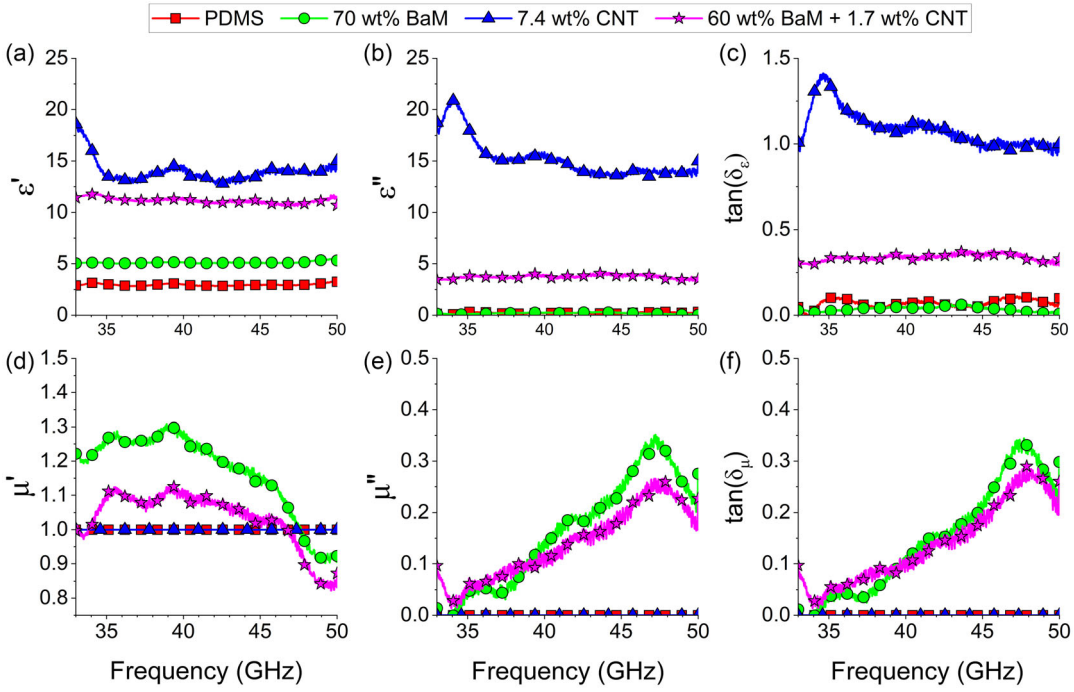

Figure 6. Electromagnetic material parameters determined using the NRW method for the following composites: 100% PDMS, 70 wt% BaM, 7.4 wt% CNT, 60% BaM + 1.7% CNTs. a) The real relative permittivity, b) imaginary relative permittivity, c) dielectric loss tangent, d) real relative permeability, e) imaginary relative permeability, and f) magnetic loss tangent.

FMR, and is less than unity above FMR. The imaginary part peaks at the FMR frequency indicating a peak in magnetic loss.

Another more relative way to display the losses is through the loss tangents plotted in Figure 6c,f. The loss tangents are defined as follows:

$$\tan(\delta_\varepsilon) = \frac{\varepsilon''}{\varepsilon'} \tag{6}$$

$$\tan(\delta_\mu) = \frac{\mu''}{\mu'} \tag{7}$$

The electrical losses come primarily from the addition of CNTs, as the PDMS and BaM nanoparticles are significantly less conductive in comparison. The magnetic losses come entirely from the BaM FMR response, as BaM is the only magnetic material present.

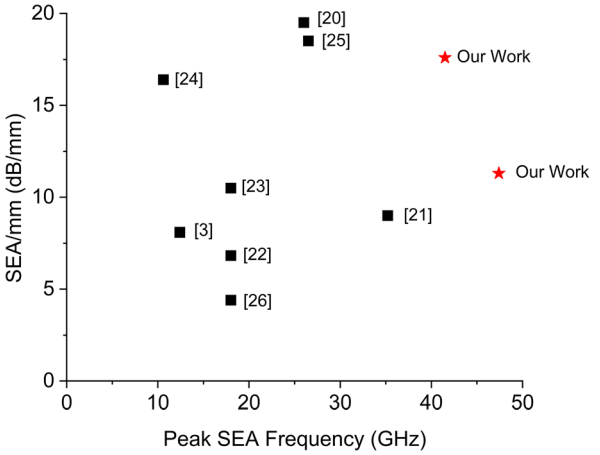

Figure 7. Plot of comparison to other microwave shielding composite materials.

4. Comparison to Other Composites in the Literature

Table 2 shows EMI shielding composites found in the literature and lists the best composite for each reference. These composites are compared graphically in **Figure 7**. Notable parameters include peak SEA, peak SEA frequency, composite thickness, and the normalized absorption is dB/mm, i.e., our FoM which allows for direct comparison between these composites. Due to the lack of a clear absorption peak from the broadband behavior of the 7.4 wt% CNT sample, the center frequency of the measured spectrum (41.5 GHz) is listed as the peak SEA frequency. Among the composites in Table 2, our composites have the highest working frequencies. Composites with higher frequencies of peak absorption are valuable, as they can be utilized in next generation communications, i.e., 5 and 6 G. However, EMI exists across the entire electromagnetic spectrum, so a higher peak absorption frequency does not necessarily make a composite superior. Our composites show very high normalized absorption, with the 7.4 wt% CNT composite having an average 17.6 dB mm^{-1} across the measured spectrum and the 60 wt% BaM + 1.7 wt% composite having a peak of 11.3 dB mm^{-1}. No other composite listed had normalized absorption of that magnitude at the high of frequency.

5. Conclusion

PDMS-based composites with added BaM nanoparticles and CNTs have been fabricated and characterized for the purpose of EMI absorption in the Q band (33–50 GHz). PDMS was chosen due to its use in microwave applications and its ability to serve as a matrix for nanoparticles. BaM was chosen for its FMR response in the microwave range, resulting in an absorption peak. CNTs were chosen for their broadband absorption due to added electrical conductivity. The fabrication process proved to be inexpensive with commercially available materials, relatively fast at around 3 h, and low temperature with the highest temperature being 80 °C.

The two most notable composites in terms of absorption presented in this work consist of 7.4 wt% CNT and 60 wt% BaM + 1.7 wt% CNT. The 7.4 wt% CNT composite demonstrates very high broadband absorption with a mean of 17.6 dB mm^{-1} across the measured spectrum. The 60 wt% BaM + 1.7 wt%

Table 2. Table of comparison to other Microwave shielding composite materials.

Reference	Composite	Composite Thickness [mm]	Maximum |SEA| [dB]	Measured Frequency Range [GHz]	Peak SEA Frequency [GHz]	Normalized SEA [dB mm^{-1}]
[3]	40 wt% BaM + 20 wt% CNT + 40 wt% PANI	4.5	36.4	8.2–12.4	12.4	8.1
[20]	Aerogel + 2.08 wt% CNT + 0.69 wt% rGO	2	39	18–26	26	19.5
[21]	Epoxy + 20 vol% AlCoCrFeNi Alloy	2	18	26.5–40	35.2	9
[22]	Paraffin wax + 8 wt% Lead Hexaferrite + 42 wt% PANI	3	20.5	8–18	18	6.8
[23]	PVA + 25 wt% Carbon Black + 35 wt% BaM	2	21	8–18	18	10.5
[24]	95% (BaM + PANI + CNT) + 5 wt% rGO	1	16.4	8.2–12.4	10.6	16.4
[25]	PEK + 20 wt% CNF	2	37	26.5–40	26.5	18.5
[26]	Polymer Blend + 2 wt% CNT + 5 wt% BaM	5	22	8–18	18	4.4
Our Work	PDMS + 7.4 wt% CNT	2.42	40.1	33–50	41.5 (center frequency)	17.6
Our Work	PDMS + 60 wt% BaM + 1.7 wt% CNT	2.42	26.9	33–50	47.4	11.3

CNT composite demonstrates high frequency-selective absorption with a peak of 11.3 dB mm^{-1} at 47.4 GHz, the FMR frequency of BaM. This frequency-selectivity results in a band-stop behavior for EMI shielding, as certain frequencies are absorbed while others are passed. Additionally, both composites reflect 5 dB of power or less, with thicker samples absorbing significantly more power than they reflect. These absorbing composites can be employed at higher frequencies than commonly found in the literature and have potential applications in shielding 5 G devices as a result.

Beyond characterizing shielding effectiveness, this rectangular waveguide method allows for the employment of the NRW method to characterize the frequency-dependent complex permittivity and permeability. The NRW method breaks down the different loss mechanisms that drive absorption and allows for the investigation of both dielectric and magnetic behavior, including FMR.

Acknowledgements

This work was supported in part by the National Science Foundation (NSF) I/UCRC on Multi-functional Integrated System Technology (MIST Center) IIP-1939009. The authors thank the staff of the Herbert Wertheim College of Engineering Research Service Centers for their assistance in the material imaging.

Conflict of Interest

The authors declare no conflict of interest.

Author Contributions

B.M.M. designed and performed the experiments, analyzed the data, and wrote the paper. F.M.F. fabricated all measured samples presented. Y.-K.Y. assisted with providing direction of the study. D.P.A. conceived and directed the study. All authors approved the final paper.

Data Availability Statement

The data that support the findings of this study are available from the corresponding author upon reasonable request.

Keywords

barium ferrite, carbon nanotubes, electromagnetic interference, ferromagnetic resonance, millimeter wave

Received: January 12, 2024
Revised: March 20, 2024
Published online: April 1, 2024

[1] L. Mohan, M. Setty, S. Karakkad, S. T. Krishnan, *IEEE Trans. Nanotechnol.* **2021**, *20*, 61.
[2] O. S. Yakovenko, L. Y. Matzui, L. L. Vovchenko, V. V. Oliynyk, V. V. Zagorodnii, S. V. Trukhanov, A. V. Trukhanov, *Nanomaterials* **2021**, *11*, 2873.
[3] M. H. Zahari, B. H. Guan, E. M. Cheng, M. F. Che Mansor, K. C. Lee, *Prog. Electromagn. Res. M* **2016**, *52*, 79.
[4] J. W. Gooch, J. K. Daher, *Electromagnetic Shielding and Corrosion Protection for Aerospace Vehicles*, Springer New York, New York, NY **2007**, https://doi.org/10.1007/978-0-387-46096-3.
[5] D. M. Pozar, *Microwave Engineering*, 4th ed., John Wiley & Sons, Hoboken, NJ **2011**, pp. 31–35.
[6] V. K. Chakradhary, M. J. Akhtar, in *2019 IEEE Asia-Pacific Microwave Conf. (APMC)*, IEEE, Piscataway, NJ, December 2019, pp. 986–988, https://doi.org/10.1109/APMC46564.2019.9038525.
[7] N. Rosdi, R. S. Azis, I. Ismail, N. Mokhtar, M. M. Muhammad Zulkimi, M. S. Mustaffa, *Sci. Rep.* **2021**, *11*, 15982.
[8] D. Mu, Z. Chen, T. Liu, Z. He, Y. Zhang, H. Yang, X. Zuo, J. Ouyang, *Mater. Chem. Phys.* **2021**, *267*, 124606.
[9] H. Lee, S. H. Ryu, S. J. Kwon, J. R. Choi, S. Bok Lee, B. Park, *Nanomicro. Lett* **2023**, *15*, 76.
[10] R. Bowrothu, H. I. Kim, C. S. Smith, D. P. Arnold, Y. K. Yoon, *IEEE Trans. Microw. Theory Tech.* **2020**, *68*, 5065.
[11] V. G. Harris, *Modern Ferrites: Emerging Technologies and Applications*, Vol. *2*. John Wiley & Sons, Hoboken, NJ **2022**, pp. 205–309.
[12] A. Ghasemi, S. Javadpour, X. Liu, A. Morisako, *IEEE Trans. Magn.* **2011**, *47*, 4310.
[13] L. Chao, A. Sharma, M. N. Afsar, *IEEE Trans. Magn.* **2012**, *48*, 2773.
[14] C. S. Smith, R. Bowrothu, Y. Wang, F. Herrault, Y. K. Yoon, D. P. Arnold, *IEEE Trans. Magn.* **2021**, *57*, pp. 1–5. https://doi.org/10.1109/TMAG.2021.3104468.
[15] A. M. Nicolson, G. F. Ross, *IEEE Trans. Instrum. Meas.* **1970**, *19*, 377.
[16] W. B. Weir, *Proc. IEEE* **1974**, *62*, 33–36.
[17] A. N. Vicente, G. M. I. Dip, C. Junqueira, in *SBMO/IEEE MTT-S Inter. Microwave and Optoelectronics Conf. Proc.*, IEEE, Piscataway, NJ **2011**, pp. 738–742. https://doi.org/10.1109/IMOC.2011.6169318.
[18] P. Galvin, Investigation of Magnitude and Phase Errors in Waveguide Investigation of Magnitude and Phase Errors in Waveguide Samples for the Nicolson-Ross-Weir Permittivity Technique Samples for the Nicolson-Ross-Weir Permittivity Technique, 2016, https://scholars.unh.edu/thesis (accessed: March 2024).
[19] J. Li, P. C. Ma, W. S. Chow, C. K. To, B. Z. Tang, J. K. Kim, *Adv. Funct. Mater.* **2007**, *17*, 3207.
[20] D. Liu, Q.-Q. Kong, H. Jia, L.-J. Xie, J. Chen, Z. Tao, Z. Wang, D. Jiang, C.-M. Chen, *Carbon N Y* **2021**, *183*, 216.
[21] Y. Zhang, B. Zhang, K. Li, G. L. Zhao, S. M. Guo, *J. Alloys Compd.* **2018**, *734*, 220.
[22] H. K. Choudhary, S. P. Pawar, S. Bose, B. Sahoo, in *AIP Conf. Proc.*, American Institute of Physics Inc., Melville, NY **2018**. https://doi.org/10.1063/1.5033126.
[23] S. Kumar, G. Datt, A. Santhosh Kumar, A. C. Abhyankar, *J. Appl. Phys.* **2016**, *120*, 164901.
[24] G. P. Abhilash, D. Sharma, S. Bose, C. Shivakumara, *Heliyon* **2023**, *9*, E13648.
[25] S. S. Chauhan, M. Abraham, V. Choudhary, *J. Mater. Sci.* **2016**, *51*, 9705
[26] S. Biswas, G. P. Kar, S. Bose, *ACS Appl. Mater. Interfaces*, **2015**, *7*, 25448